ISSN 1063-7842, Technical Physics, 2018, Vol. 63, No. 9, pp. 1311–1315. © Pleiades Publishing, Ltd., 2018.
Original Russian Text © A. Krylov, S. Krylova, S. Kopyl, A. Kholkin, 2018, published in Zhurnal Tekhnicheskoi Fiziki, 2018, Vol. 88, No. 9, pp. 1355–1358.

DEVELOPMENT OF PROCESS TECHNOLOGIES, DIAGNOSTIC METHODS, AND FUNCTIONAL MATERIALS AND STRUCTURES

Non-Hydrostatic Pressure-Induced Phase Transitions in Self-Assembled Diphenylalanine Microtubes

A. Krylov[a,*], S. Krylova[a], S. Kopyl[b], and A. Kholkin[b]

[a] *Kirensky Institute of Physics, Krasnoyarsk Scientific Center, Siberian Branch, Russian Academy of Sciences, Krasnoyarsk, 660036 Russia*

[b] *University of Aveiro, Materials Institute of Aveiro, Department of Physics & CICECO, Aveiro, 3810-193 Portugal*

**e-mail: slanky@iph.krasn.ru*

Received December 18, 2017

Abstract—The structural phase transitions in diphenylalanine microtubes caused by an increase in the non-hydrostatic pressure have been examined. Raman scattering investigations have been carried out and the results obtained have been interpreted and analyzed. Spectral variations in the ranges of phenyl ring vibrations and high-frequency oscillations of NH and CH groups have been analyzed. Under pressures of up to 9.8 GPa, four spectral anomalies indicative of the occurrence of phase transitions have been observed. The transitions under pressures of 1.7 and 4 GPa are shown to be reversible. The transition at 5.7 GPa is accompanied by partial sample amorphization.

DOI: 10.1134/S1063784218090098

Peptides attract attention of researchers by their biocompatibility and unique biological and physical properties. The shortest peptide sequence is diphenylalanine. Diphenylalanine self-assembles with the formation of derivative dipeptide nanostructures, including tubes, spheres, plates, and hydrogels [1]. Such structures are characterized by the very high temperature and chemical stability [2]. Peptide nanotubes exhibit unique properties, which make it possible to use them as main nanoelectronic elements. Among these properties are the piezo- and pyroelectric effects [1–4]. This material has been already used in piezoelectric resonators, microsolenoids, and batteries [1, 5–7]. In addition, the attention of researchers has been attracted by the materials with new intriguing properties synthesized by compression of peptide microtubes [8]. The aim of this work was to investigate possible structural phase transitions occurring in diphenylalanine microtubes under high pressure. It is worth noting that Raman scattering of light is widely used in studying structural phase transitions [8–12]; therefore, we used this technique in the present work.

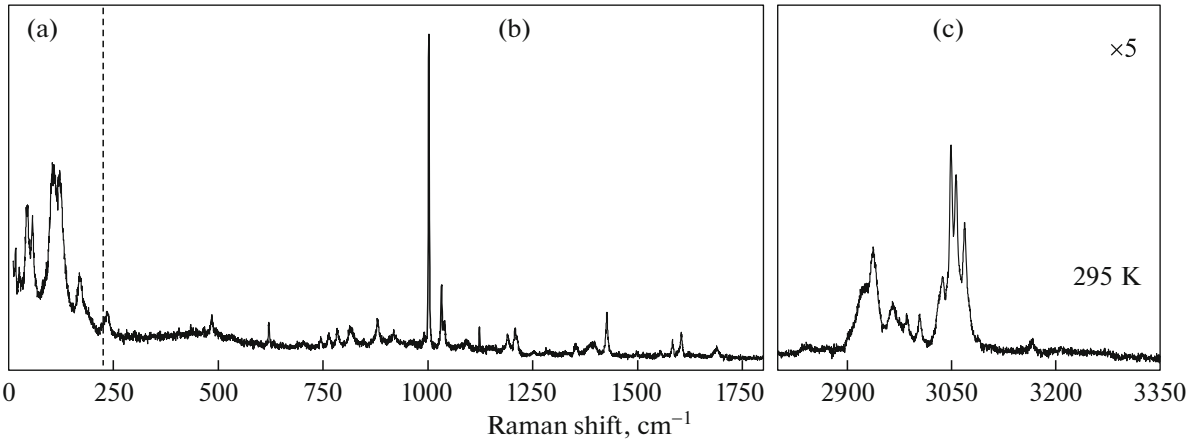

Fig. 1. Full Raman scattering spectrum at a temperature of $T = 295$ K and normal atmospheric pressure ($P = 0$ GPa).

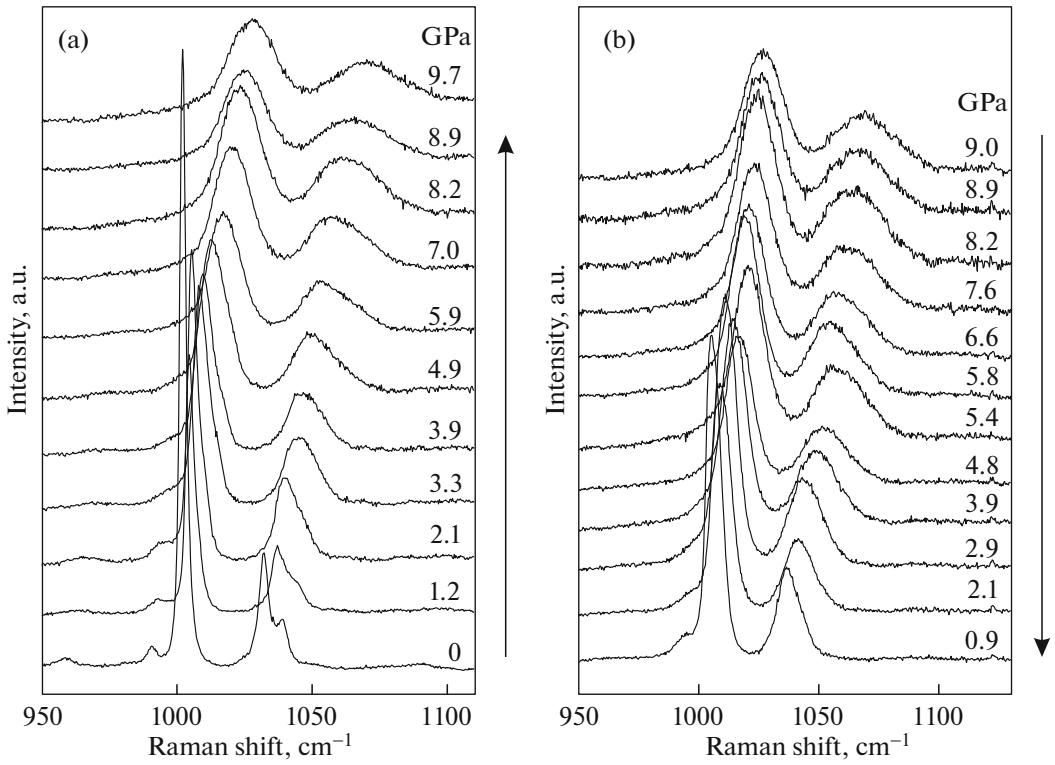

Fig. 2. Spectrum transformation in the phenyl ring vibration range with (a) increasing and (b) decreasing pressure.

In recording Raman spectra, the polarized Ar^+ laser radiation with a wavelength of 514.5 nm was used as an excitation source. The spectra in the 180° geometry were obtained on a Horiba Jobin Yvon T64000 spectrometer. The high-pressure experiments were conducted at a temperature of 295 K in a Diacell μScopeDAC-HT(G) high-pressure cell. The pressure was determined from a shift of the $^5D_0$–$^7F_0$ luminescence band of the Sm^{2+} samarium ion in the SrB_4O_7 : Sm^{2+} crystal [13–15]. The pressure determination error was about 0.05 GPa.

The organic crystal belongs to the sp. gr. $P6_1$ [17]. The cell includes six NH_2PhePheCOOH molecules, each containing 43 ions localized in Wyckoff position 6a. The selection rules at the Brillouin zone center are $\Gamma_{\text{Raman}} = 128A + 129^1E_2 + 129^2E_2 + 128^1E_1 + 128^2E_1$ for Raman scattering and $\Gamma_{\text{IR}} = 128A + 128^1E_1 + 128^2E_1$ for infrared absorption; the acoustic modes are $\Gamma_{\text{Ac}} = A + {}^1E_1 + {}^2E_1$, where $^1E_2$, $^2E_2$ and $^1E_1$, $^2E_1$ are the complex conjugate representations of the longitudinal and transverse modes. Inside nanochannels, there are also water molecules [17].

Figure 1 shows the full Raman scattering spectrum at a temperature of $T = 295$ K. The spectrum can be divided into three regions corresponding to vibrations of the structural elements: (a) 10–220 cm^{-1} correspond to the lattice vibrations; (b) 220–1800 cm^{-1}, to the internal vibrations of groups including COO and C–C; the line 1002 cm^{-1} corresponding to the phenyl ring breathing mode; the lines 1032 cm^{-1} correspond to the deformation vibrations of C–H groups and vibrations of NH_3 groups; and (c) lines 2800–3250 cm^{-1} correspond to the stretching vibrations of C–H and N–H groups [8].

The line 1002 cm^{-1} corresponds to the breathing vibrations of the aromatic ring. This line has the highest intensity in the spectrum. The changes in this spectral region with increasing and decreasing pressure are illustrated in Figs. 2a and 2b, respectively. As the pressure decreases, the spectra are not exactly repeated, which is indicative of irreversibility of the structural changes. To follow the changes in the spectrum, we established pressure dependences of the line shift (Fig. 3a) and width (Fig. 3b). Closed triangles show positions (Fig. 3a) and widths (Fig. 3b) of the line 1036 cm^{-1}; closed circles, positions (Fig. 3a) and widths (Fig. 3b) of the line 1032 cm^{-1}; and open squares, positions (Fig. 3a) and widths (Fig. 3b) of the line 1002 cm^{-1}. Closed upside-down triangles show positions (Fig. 3a) and widths (Fig. 3b) of the line 1003 cm^{-1} detected upon pressure growth to 1.1 GPa. According to the behavior of these parameters, we may assume that the structural changes occur under pressures of 2, 5.7, and, possibly, 4 GPa. To establish the possible third transition, we plotted a ratio between the intensities of the lines 1002 and 1032 cm^{-1}. Figure 3c

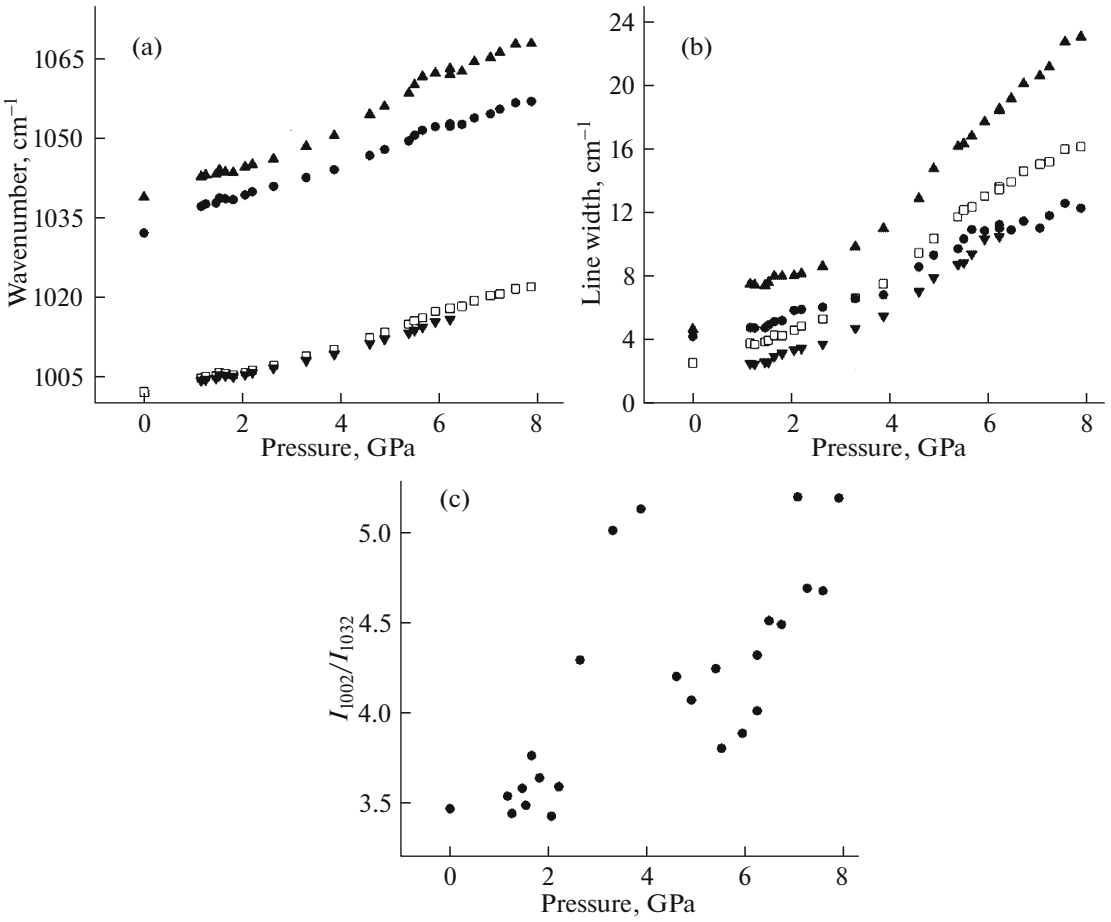

Fig. 3. Temperature dependences of (a) the line position displacement, (b) line width, and (c) ratio between the intensities in the phenyl ring vibration range.

shows the result that confirms the occurrence of phase transitions under pressures of 1.7, 4, and 5.7 GPa. The bands 1032 and 1038 cm^{-1} correspond to the in-plane phenyl-ring longitudinal vibrations. The molecule contains two almost identical aromatic rings; these two vibrations are split in the spectrum in the presence of water. The distance between vibrations allows a number of water molecules inside the ring from 6 diphenylalanine molecules to be estimated [17]. The behavior of the distance between these two peaks is illustrated in Fig. 4. It can be seen that the distance between the peaks decreases to 1.7 GPa, then starts growing to 4 GPa, and after that continues growing, but with the change in the curve slope. The slope changes at 5.7 GPa are also indicative of a phase transition.

In the high-frequency spectral range corresponding to the vibrations of C–H and N–H groups, one can also observe the changes related to the phase transitions. Figure 5a shows spectrum transformations with increasing pressure. Under normal conditions (without pressure), seven lines are observed. As the pressure grows, two broad lines remain in the spectrum. Figure 5b presents the pressure dependence of line positions. Dashed lines show the spectroscopic changes indicative of the occurrence of phase transitions, specifically, the change in the number of lines

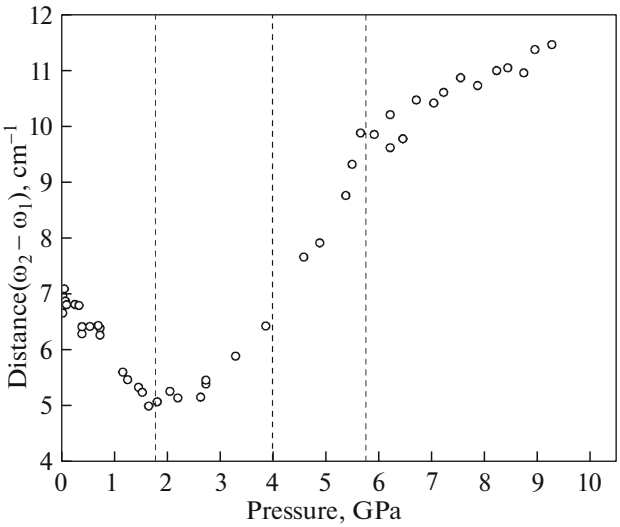

Fig. 4. Distance between the peaks ω_1 = 1032 cm^{-1} and ω_2 = 1038 cm^{-1} as a function of pressure.

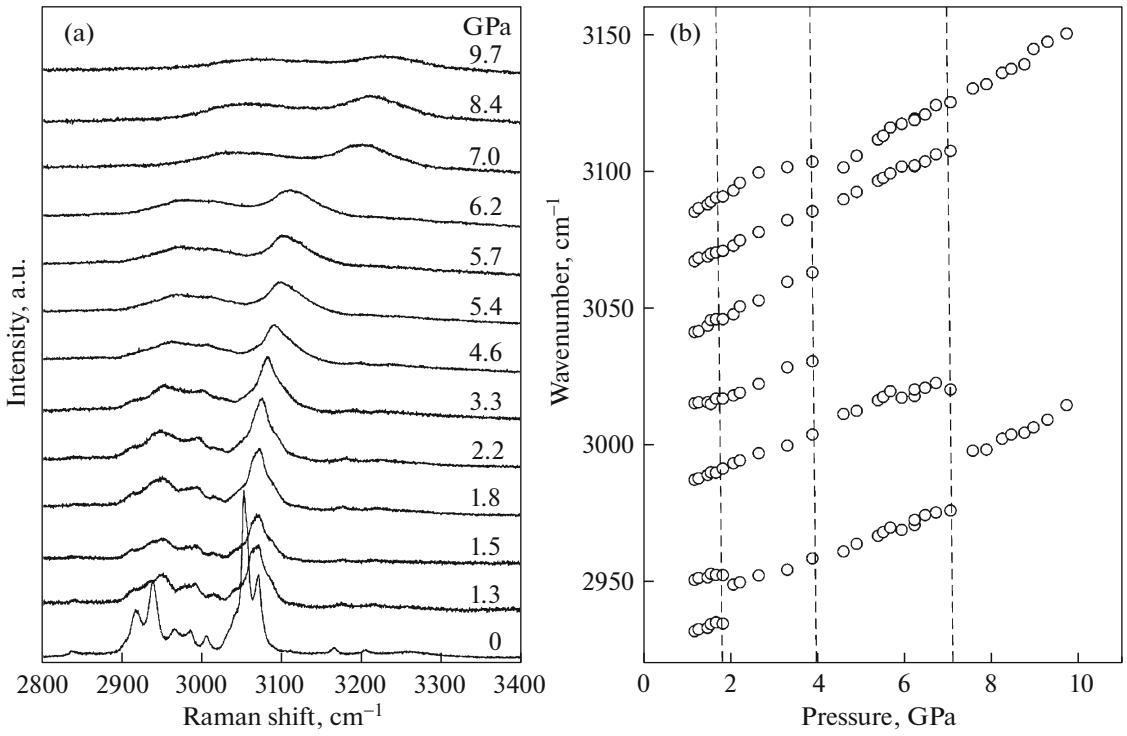

Fig. 5. High-frequency vibrations: (a) transformation of the spectra with increasing pressure and (b) pressure dependence of the line position displacement.

and slope of the line position displacement. The changes in the spectra point out the occurrence of the fourth phase transition under a pressure of $P_4 = 7$ GPa (Fig. 5b).

The experimental observations revealed four critical points under pressures of $P_1 = 1.7$, $P_2 = 4$, $P_3 = 5.7$, and $P_4 = 7$ GPa. Prior to the first critical point, the tubes were compressed without the crystal structure destruction. The first and second phase transitions are reversible. Nevertheless, even the pressure growth above 6 GPa did not lead to complete amorphization. The number of phase transitions observed in this work is larger than in study [9]. This is due to the fact that we investigated a wider pressure range upon nonhydrostatic compression. In addition, we examined the high-frequency spectral ranges corresponding to the vibrations of C–H and N–H groups, which were not studied in detail in [9]. The data obtained by us can be used to synthesize new materials and understand the fundamentals of physical properties of microtubes. However, determination of high-pressure phases of peptide tubes needs further X-ray diffraction study.

ACKNOWLEDGMENTS

This study was supported by the Turkish–Portuguese project no. TUBITAK/0006/2014.

REFERENCES

1. L. Adler-Abramovich and E. Gazit, Chem. Soc. Rev. **43**, 6881 (2014).
2. L. Adler-Abramovich, D. Aronov, P. Beker, M. Yevnin, S. Stempler, L. Buzhansky, G. Rosenman, and E. Gazit, Nat. Nanotechnol. **4**, 849 (2009).
3. A. Kholkin, N. Amdursky, I. Bdikin, E. Gazit, and G. Rosenman, ACS Nano **4**, 610 (2010).
4. A. Esin, I. Baturin, A. Nikitin, T. Vasilev, F. Salehli, V. Shur, and A. Kholkin, Appl. Phys. Lett. **109**, 142902 (2016).
5. E. D. Bosne, A. Heredia, S. Kopyl, D. V. Karpinsky, A. G. Pinto, and A. L. Kholkin, Appl. Phys. Lett. **102**, 073504 (2013).
6. A. Nuraeva, S. Vasilev, D. Vasileva, P. Zelenovskiy, D. Chezganov, A. Esin, S. Kopyl, K. Romanyuk, V. Shur, and A. Kholkin, Cryst. Growth Des. **16**, 1472 (2016).
7. K. Ryan, J. Beirne, G. Redmond, J. I. Kilpatrick, J. Guyonnet, N.-V. Buchete, A. L. Kholkin, and B. J. Rodriguez, ACS Appl. Mater. Interfaces **7**, 12702 (2015).
8. P. S. Zelenovskiy, A. O. Davydov, A. S. Krylov, and A. L. Kholkin, J. Raman Spectrosc. **48**, 1401 (2017).
9. J. G. da Silva Filho, J. Mendes Filho, F. E. A. Melo, J. A. Lima, and P. T. C. Freire, Vib. Spectrosc. **92**, 173 (2017).
10. A. S. Krylov, S. V. Goryainov, N. M. Laptash, A. N. Vtyurin, S. V. Melnikova, and S. N. Krylova, Cryst. Growth Des. **14**, 374 (2014).

11. A. N. Vtyurin, A. S. Krylov, S. V. Goryainov, S. N. Krylova, A. S. Oreshonkov, and V. N. Voronov, Phys. Solid State **54**, 934 (2012).
12. A. N. Vtyurin, S. V. Goryalnov, N. G. Zamkova, V. I. Zinenko, A. S. Krylov, S. N. Krylova, Comput. Mater. Sci. **36**, 79 (2006).
13. I. K. Bdikin, V. Bystrov, S. Kopyl, R. Lopes, I. Delgadillo, J. Gracio, E. Mishina, A. Sigov, and A. L. Kholkin, Appl. Phys. Lett. **100**, 043702 (2012).
14. A. S. Krylov, I. Gudim, I. Nemtsev, S. N. Krylova, A. V. Shabanov, and A. A. Krylov, J. Raman Spectrosc. **48**, 1406 (2017).
15. A. Pugachev, I. Zaytseva, A. Krylov, V. Malinovsky, N. Surovtsev, Yu. Borzdov, and V. Kovalevsky, Ferroelectrics **508**, 161 (2017).
16. C. H. Görbitz, Chem. Commun., No. 22, 2332 (2006).
17. X. Wu, S. Xiong, M. Wang, J. Shen, P. K. J. Chu, Phys. Chem. C **116**, 9793 (2012).

Translated by E. Bondareva